Phys. Biol. **5** (2008) 016002 (10pp) doi:10.1088/1478-3975/5/1/016002

Predicting ribosomal frameshifting efficiency

Song Cao and Shi-Jie Chen

Department of Physics and Department of Biochemistry, University of Missouri-Columbia, Columbia, MO 65211, USA

E-mail: chenshi@missouri.edu

Received 19 December 2007
Accepted for publication 18 February 2008
Published 10 March 2008
Online at stacks.iop.org/PhysBio/5/016002

Abstract

Many retroviruses use −1 ribosomal frameshifting as part of the mechanism in translational control of viral protein synthesis. Quantitative prediction of the efficiency of −1 frameshifting is crucial for understanding the viral gene expression. Here we investigate the free energy landscape for a minimal −1 programmed ribosomal frameshifting machinery, including the codon–anticodon base pairs at the slippery site, the downstream messenger RNA structure and the spacer between the slippery site and the downstream structure. The free energy landscape analysis leads to a quantitative relationship between the frameshifting efficiency and the tension force generated during the movement of codon–anticodon complexes, which may occur in the A/T to A/A accommodation process or the translocation process. The analysis shows no consistent correlation between frameshifting efficiency and global stability of the downstream mRNA structure.

Introduction

For many viruses, the translational control of viral proteins is regulated by an endogenous −1 programmed ribosomal frameshifting (−1 PRF) [1–10]. −1 PRF is responsible for producing the gag-pol protein [11]. Maintaining a normal ratio of gag and gag-pol proteins is critical for the replication and viability of the retroviruses [12]. Slight alteration in the frameshifting efficiency can result in the reduction or elimination of virus production. The pseudoknot in the (3′) downstream messenger RNA (mRNA) plays a unique role in promoting −1 PRF [13]. Experiment found that the simple stem-loop structure cannot replace the pseudoknot to induce the efficient frameshifting [14, 15] for many viruses. A mechanical model was proposed to explain the mechanism of −1 PRF induced by the pseudoknot [16]. In the mechanical model, the proposed process of −1 PRF involves three steps, as follows. (i) The downstream pseudoknot is blocked at the entrance of the downstream tunnel, which results in the stalling and pausing of the elongating ribosome over the slippery sites. (ii) Upon the coupled accommodation of tRNA and mRNA from the A/T hybrid state to the A/A state, the anticodon loop of the aa-tRNA along with the mRNA chain moves 9 Å in the 5′ direction, generating a tension force in the single-stranded mRNA spacer between the A-site and the downstream structure at the entrance of the ribosome tunnel. The tension stretches both the codons and the downstream structure (usually pseudoknot), causing the shift of the codons in the 3′ direction if the downstream structure is sufficiently stable against the tension force. (iii) The downstream pseudoknot is unfolded by the elongating ribosome, and the translation proceeds in the new −1 frame.

When the −1 ribosomal frameshifting happens, a single nucleotide originally in the codon region enters the spacer, resulting in a relaxation of the tension in the spacer. The release of the tension helps stabilizing the system in the new reading frame. Alternatively, the tension force in the spacer can cause unfolding of the downstream structure (pseudoknot), which can also relax the tension. Therefore, in order for the frameshifting to occur, the downstream structure must be sufficiently stable against the tension force. Such a mechanical stability is in contrast to the thermal stability of the global structure.

Most of the efficient frameshifting involves the formation of a pseudoknot structure [4, 5, 10]. However, in human immunodeficiency virus (HIV)-1 type B, recent NMR studies [17, 18] showed that a two-stem structure is responsible for the efficient frameshifting, which is consistent with the

biochemical analysis by Dulude *et al* [19]. A simple stem-loop structure was originally proposed by Jack *et al* [20]. Subsequent studies found that the structure was more complex than a simple stem-loop structure. Du *et al* [21], Taylor *et al* [22] and Baril *et al* [23] proposed a pseudoknot instead of stem-loop. Dinman *et al* proposed an intramolecular triplex RNA structure [24]. In addition, in HIV-1 type B, the spacer length is quite unique. Usually, the spacer length is ranged from 5 nucleotide (nt) to 8 nt in a pseudoknot-induced frameshifting system [7, 8]. However, the spacer in the HIV-1 type B frameshifting system contains only one nucleotide [17–19].

The mechanism of frameshifting can involve complicated interactions between mRNA, ribosome, tRNA and other cofactors. Experimental studies provided great insights into the mechanism of frameshifting. However, different experiments on different frameshifting systems can sometimes lead to different models, revealing different aspects of the frameshifting mechanism. For instance, a recent single-molecule experiment [25, 26] on the mechanical property of the frameshifting system led to the conclusion that frameshifting efficiency may be correlated to the unfolding kinetics of the downstream pseudoknot [27]. In addition, biochemical studies suggested that frameshifting efficiency can be correlated to the stability of the mRNA pseudoknot [7, 28, 29], and loop-stem tertiary interactions in the pseudoknot can be important to determine the frameshifting efficiency [6, 29]. In contrast, a mechanical model suggested that the frameshifting efficiency may be correlated to the tension force in the spacer region [16, 30, 31]. Several mechanisms have been proposed on how and when such frameshifting-stimulatory tension force is generated. Depending on the different models for the occurrence of the tension, frameshifting can occur either co-translocationally [30, 31] or immediately after aa-tRNA accommodation from A/T to A/A state [16]. Brierley *et al* [30] and Brakier-Gingras *et al* [31] proposed that frameshifting can occur during translocation. The electron cryo-microscopy (cryo-EM) [30] shows that the translocation of the eEF2 ribosome generates a strain on the tRNA P site which may promote the ribosomal frameshifting.

Here we investigate the free energy landscape for a coupled three-component minimal frameshifting machinery (codon–anticodon region, spacer and the downstream structure). The results support the correlation between the frameshifting efficiency and the tension force during the movement of the codon–anticodon complexes. Such movement can be realized during the accommodation process [16] or the translocation process [30]. In the present study, we neglect the protein–mRNA interaction since previous experiments suggested that protein might not be a determining factor for frameshifting [32, 33].

Our results are based on a specific model that tension-driven frameshifting occurs during the movement of the codon–anticodon complex. Extensive tests against experiments show good quantitative agreements between our theory and experiment. However, due to the complexity of the system, our theory does not exclude other possibilities for the frameshifting mechanism, such as the kinetic effects

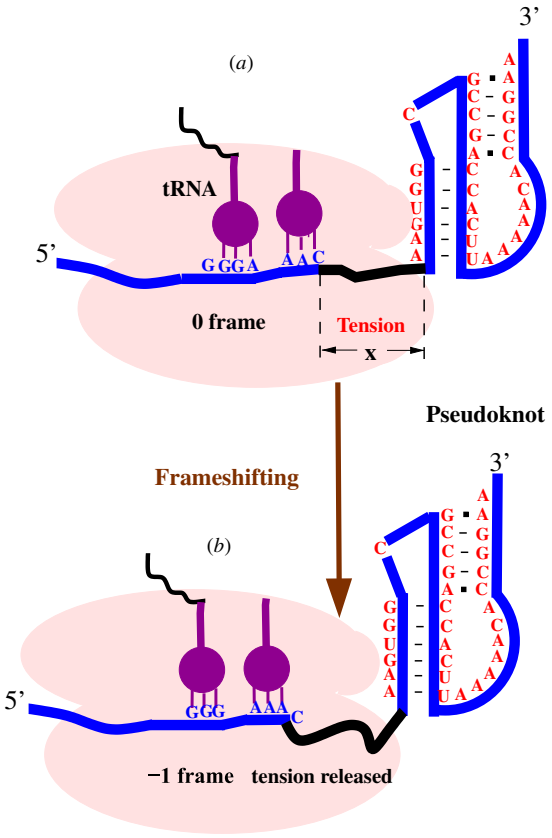

Figure 1. A schematic diagram for the −1 ribosomal frameshifting induced by the ScYLV pseudoknot (with blue backbone) [29]. When the −1 ribosomal frameshifting occurs, the slippery region of mRNA (blue) is shifted in the 5′ → 3′ direction by one nucleotide, causing the reading form to be shifted from the original 0 frame (*a*) to the new shifted −1 frame (*b*). Upon the frameshifting, the tension in the spacer of mRNA (black) is released.

[27] and the loop-stem tertiary interactions in the stimulatory pseudoknot. For instance, our model underestimates the frameshifting efficiency for sugarcane yellow leaf virus (ScYLV) pseudoknot because the model does not account for the loop-stem tertiary interactions [29]. It is highly possible that the PRF efficiency is determined by multiple factors and our model captures certain aspects of the complete mechanism.

Materials and methods

A ribosomal frameshifting machinery consists of three essential components (figure 1): (i) the mRNA slippery sites which form base pairs with tRNA, (ii) a spacer usually having a length ranging from 5 nt to 8 nt and (iii) usually a pseudoknot structure adjacent to the 3′ end of the spacer. The slippery site contains a heptamer sequence XXXYYYZ, where X can be any nucleotide, Y is adenosine (A) or uridine (U) and Z is A, U or cytidine (C) [1]. In the 0 frame, the translated codons are (XXY, YYZ). In the −1 frame, the codons are changed to (XXX, YYY). The relative population of the 0 frame and the −1 frame determines the production of different proteins (*gag* and *gag-pol*).

We describe a state of the above three-component system using two parameters: (a) m = the number of unpaired nucleotides in the spacer, i.e. the length of the spacer, and (b) X = the end-to-end distance (extension) of the spacer. For a given state (m, X), the partition function of the system is equal to

$$Q_{\mathrm{PRF}}(m, X) = Q_{\mathrm{codon}} Q_{ss}(m, X) Q_{ds},$$

where Q_{codon}, $Q_{ss}(m, X)$ and $Q_{ds}(m)$ are the partition functions of the codon–anticodon base-pairing duplex (in the slippery region), of the (single-stranded) spacer and of the 3′ downstream mRNA structure ('structured' region, excluding the 5′ and 3′ tails). The free energy landscape of the three-component system is determined by the following equation:

$$\Delta G_{\mathrm{PRF}}(m, X) = \Delta G_{\mathrm{codon}} + \Delta G_{ss}(m, X) + \Delta G_{ds}, \qquad (1)$$

where $\Delta G_i = -k_{\mathrm{B}} T \ln Q_i$ is the free energy of system i (='PRF', 'codon', 'ss', 'ds').

Free energy of the 3′ downstream mRNA structure

We compute ΔG_{ds} from the partition function given by the sum over all the possible structures:

$$\Delta G_{ds} = -k_{\mathrm{B}} T \ln \sum_{\mathrm{struct}} \mathrm{e}^{-\Delta G_{\mathrm{struct}}/k_{\mathrm{B}} T},$$

where $\Delta G_{\mathrm{struct}}$ is the free energy of a structure. In our conformational ensemble, we consider all the possible secondary structures, pseudoknotted structures. We use the previously developed *Vfold* model to compute $\Delta G_{\mathrm{struct}}$ for the secondary structures [34, 35] and pseudoknots [36].

Free energy of the codon–anticodon base-pairing duplex

We use the Turner rules and the nearest neighbor model [37] to calculate the free energy ($\Delta G_{\mathrm{codon}}$) for the two 3-base pair (bp) codon–anticodon duplexes [38] (figures 1(*a*) and (*b*)). For example, in the 0 frame (figure 1(*a*)), the two 3-bp duplexes are 5′(GGA)-(UCC)3′ and 5′(AAC)-(GUU)3′, with free energy ($T = 25\ ^\circ$ C) equal to $\Delta G^{(0)}_{\mathrm{codon}} = 5'\mathrm{GG} - \mathrm{CC3}' + 5'\mathrm{GA} - \mathrm{UC3}' + 5'\mathrm{AA} - \mathrm{UU3}' + 5'\mathrm{AC} - \mathrm{GU3}' = -9.5$ kcal mol^{-1}. Similarly, in the (shifted) -1 frame (figure 1(*b*)), the two 3-bp duplexes are 5′(GGG)-(UCC)3′ and 5′(AAA)-(GUU)3′, with free energy ($T = 25\ ^\circ$ C) equal to $\Delta G^{(-1)}_{\mathrm{codon}} = 5'\mathrm{GG} - \mathrm{CC3}' + 5'\mathrm{GG} - \mathrm{UC3}' + 5'\mathrm{AA} - \mathrm{UU3}' + 5'\mathrm{AA} - \mathrm{GU3}' = -7.8$ kcal mol^{-1}. The base pairs in the -1 frame is less stable by 1.7 kcal mol^{-1} than in the 0 frame for the ScYLV frameshifting system in figure 1.

Free energy of a (single-stranded) spacer

For the spacer region which is single stranded, the free energy can be evaluated from the elastic energy (=the work done by the intrinsic elastic force):

$$\Delta G_{ss}(m, X) = \int_0^X f_{ss}(X')\, \mathrm{d}X', \qquad (2)$$

where (m, X) is the (chain length, end–end distance) of the spacer and f_{ss} is the elastic force, which can be determined from the extensible freely jointed chain model (EFJC) [39–44]:

$$X(f_{ss}) = m L_{ss} \left[\coth\left(\frac{f_{ss} b}{k_B T}\right) - \frac{k_B T}{f_{ss} b} \right] \left[1 + \frac{f_{ss}}{S} \right]. \qquad (3)$$

We use Kuhn length $b = 1.5$ nm and base-to-base distance $L_{ss} = 0.56$ nm along the chain for RNA and elastic stretch modulus $S = 800$ pN [39–41].

The free energy landscape $\Delta G_{\mathrm{PRF}}(m, X)$ gives the probability of finding the system in the (m, X) state among all the possible spacer and downstream structures. For an ensemble of conformations (of the spacer and the downstream structure), the free energy landscape gives the following ensemble-averaged properties for a given extension X of the spacer.

(1) The free energy for the system: $\Delta G_{\mathrm{PRF}}(X) = -k_{\mathrm{B}} T \ln \sum_m Q_{\mathrm{PRF}}(m, X)$.

(2) Force–extension relationship:

$$F(X) = \mathrm{d}\Delta G_{\mathrm{PRF}}(X)/\mathrm{d}X. \qquad (4)$$

In contrast to the force–extension relationship in equation (3), the above $F(X)$ is a weighted average over all the possible downstream structures for a given extension X of the spacer.

(3) The mean spacer length $\overline{m}$(X) as a measure for the unfolding level of the downstream structure:

$$\overline{m}(X) = \sum_m m Q_{\mathrm{PRF}}(m, X) \Big/ \sum_m Q_{\mathrm{PRF}}(m, X). \qquad (5)$$

(4) The probability $P_{ij}(X)$ for nucleotides i and j to form a base pair:

$$P_{ij}(X) = \sum_m Q^{(ij)}_{\mathrm{PRF}}(m, X) \Big/ \sum_m Q_{\mathrm{PRF}}(m, X). \qquad (6)$$

Here, $Q^{(ij)}_{\mathrm{PRF}}(m, X)$ is the conditional partition function for all the structures that contain a base pair (i, j).

Results and discussion

Instead of focusing only on the downstream structures as in most previous frameshifting studies, here we treat the coupling within the three-component frameshifting system. The interplay between the different factors determines the frameshifting efficiency. For instance, the frameshifting efficiency is correlated to the stability of the first few base pairs in the helix stem (of the downstream pseudoknot) where the spacer is connected and the tension force from the spacer is exerted.

We investigate the physical mechanism for three paradigm systems: ScYLV, infectious bronchitis virus (IBV) and the various mutants, and HIV-1 type O. Experimental studies indicated pseudoknot-promoted frameshifting for ScYLV [29], IBV [45, 46] and HIV-1 type O [47, 48]. We would like to understand why and how pseudoknots promote frameshifting for different mRNA sequences.

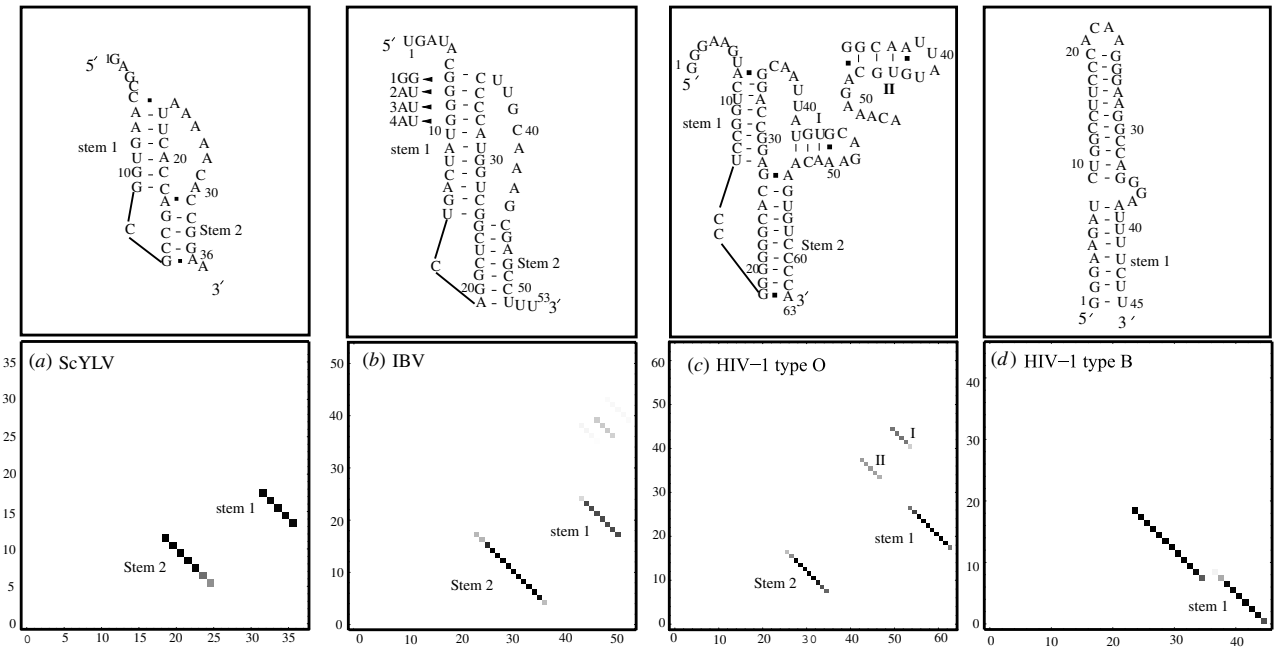

Figure 2. The predicted native structures for (*a*) ScYLV [29], (*b*) IBV [45], (*c*) HIV-1 type 0 [19] and (*d*) HIV-1 type B [17] at room temperature ($T = 25$ °C). Also shown are the density plots for the base pairing probabilities with rows and columns representing the sequences. HIV-1 type B forms a two-helix stem-loop structure and the rest form pseudoknots. We find two alternative structures (I, II) for loop 2 in HIV-1 type 0.

Native structures of the mRNA downstream pseudoknots

We first apply the previously developed *Vfold* model to predict the native structure for the mRNA sequence from the single-stranded spacer to the downstream structure region (figure 2). In the native structure calculation, the chain is treated as a (force-)free chain without the frameshifting context. We use the *Vfold* model to compute the thermal equilibrium base pairing probability [34, 49, 50]: $P_{ij} = Q_{ij}/Q_{\rm tot}$, where Q_{ij} is the conditional partition function for all the possible structures that contain the (i, j) base pair and $Q_{\rm tot}$ is the total partition function for all the possible structures (regardless of the base pairs). From P_{ij} we determine the most probable structure (figure 2). Since the helix stems in the frameshift-promoting pseudoknot are often bent [17, 51], we do not add the coaxial stability to the pseudoknot in our computation [52]. In our calculation, we adopt the mRNA frameshifting sequences used in the experimental literature [17, 29, 45, 47]. The truncated mRNA sequences between the codon–anticodon base pairs and the downstream structure (see table 1) are believed to be directly involved in frameshifting. The tension force during frameshifting is mainly determined by the first few base pairs at the terminal of stem 1 in the downstream pseudoknot. Thus, adding bases at the 3′ single-stranded end of the pseudoknot would not significantly affect the results. The predicted structures agree with the experimental results [17, 29, 45, 47]. Moreover, the predicted spacer lengths (tails in the 5′ end of the pseudoknot) in ScYLV, IBV and HIV-1 type O are 5 nt, 6 nt and 8 nt, respectively, which are within the experimentally suggested range between 5 nt and 8 nt [7]. For HIV-1 type B, our predicted structure is a stem-loop structure, which is consistent with the NMR measurement [17]. However, it should be noted that the predicted structure is in the absence of force and is not in the context of frameshifting machinery. The tension force can induce the unzipping of the lower helix, and one unzipped strand of the lower helix can potentially form the triplex structure proposed by Dinman *et al* [24]. Due to lack of the thermodynamic parameters of the triplex, we are currently unable to accurately model the free energy landscape for the triplex formation. Therefore, in the present study, we will focus on the pseudoknot-stimulated frameshifting systems.

Free energy landscape of the frameshifting system

We use the EFJC to compute the elastic free energy of the spacer region (equations (2) and (3)). The freely jointed chain (FJC) model is an approximation valid for a single-stranded chain at low force ($\leqslant$10 pN). For large force ($\geqslant$10 pN), the EFJC model [39–41], which is more general, would give a better description for the force–extension relationship. Our test results for the two models (figure 3) show that the FJC model can overestimate the tension force for the ScYLV frameshifting system. For instance, the force at peak 1 in figure 3 predicted from the FJC model is about 15 pN higher than that from the EFJC model with elastic stretch modulus $S = 800$ pN. As shown in figure 3, FJC and EFJC give the same results for large S (e.g., $S = 10^4$ pN). In the following calculations, we use the EFJC model with $S = 800$ pN [39].

We use the free energy landscape $\Delta G_{\rm PRF}(X)$ to describe the stability of the system. The use of $\Delta G_{\rm PRF}(X)$ is motivated

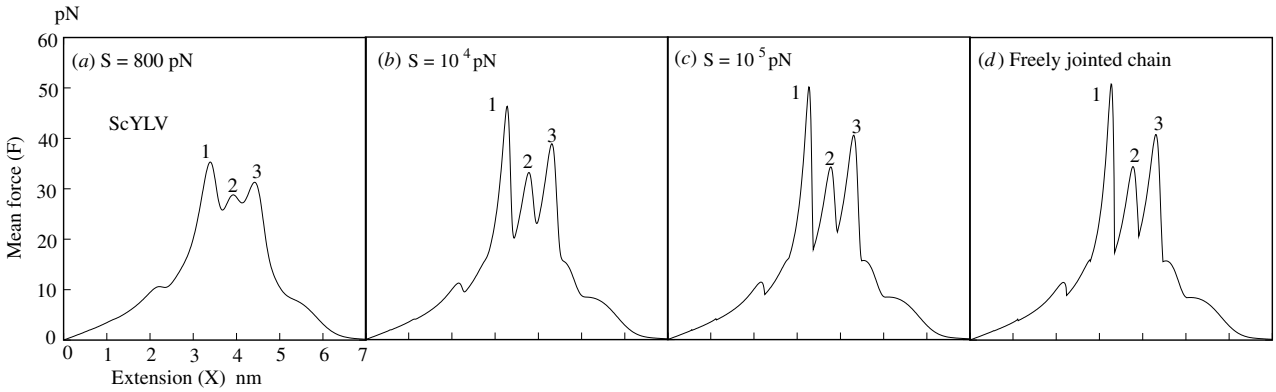

Figure 3. The force–extension curves for the ScYLV pseudoknot. We calculated the curves using the extensible freely jointed chain model. We use three different elastic stretch modulus parameters: (*a*) $S = 800$ pN, (*b*) $S = 10^4$ pN and (*c*) $S = 10^5$ pN. For very large S ($=10^5$ pN), the extensible freely jointed chain model (*c*) gives the same result as the freely jointed chain model (*d*).

Table 1. In the table, we use *Vfold* model [34, 36] to analyze the mechanical properties for ScYLV, minimal IBV and the nine mutants (pKA18, 1GG, 2AU, pKA41, 3AU, 4AU, pKA49, pKA13 and pKA9) of IBV, HIV-1 type 0 and HIV-1 type B. We show the maximum force and the average force in the region for X from 3.3 nm to 4.3 nm, corresponding to the 1 nm movement for the codon–anticodon duplex along the ribosome tunnel. The movement is supported by the 9 Å model [16]. We find a correlation between the frameshifting efficiency and the average force in the [3.3 nm, 4.3 nm] range (see also figure 7). For example, the mutant 2AU severely affects the peak force at $X = 3.3$ nm and 4.0 nm, and result in a lower average force than that of the wild-type IBV. The frameshifting efficiency is 30% less than that of the wild-type IBV. For 2AU and 4AU, we use the same frameshifting efficiency as that of pKA41 and pKA49, respectively, since it is found in the experiment that mutations beyond the fourth base pairs affect the frameshifting efficiency very weakly [45]. Indeed, we found a similar average force for 2AU and pKA41, 4AU and pKA49. The fitted analytical formula for the efficiency (η)–force relationship is $\eta \simeq 0.0083e^{0.1F_{\text{avg}}}$.

Sequence	Truncated sequence	PRF efficiency	Spacer length	Predicted structure	Average force
ScYLV [29]	G1-C36	15%	5 nt	Pseudoknot	29 pN
IBV [45]	U1-U53	48%	6 nt	Pseudoknot	38 pN
pKA18 [45]	U1-U53	48%	6 nt	Pseudoknot	40 pN
1GG [56]	U1-U53	Less 10 %	6 nt	Pseudoknot	36 pN
2AU [45]	U1-U53	Less 30%	6 nt	Pseudoknot	28 pN
pKA41 [45]	U1-U53	18 %	6 nt	Pseudoknot	28 pN
3AU	U1-U53	No experiment	6 nt	Pseudoknot	32 pN
4AU [45]	U1-U53	Less 10%	6 nt	Pseudoknot	36 pN
pKA49 [45]	U1-U53	35 %	6 nt	Pseudoknot	40 pN
pKA13 [45]	U1-U51	7%	6 nt	Pseudoknot	22 pN
pKA9 [45]	U1-C44	2%	6 nt	Pseudoknot	20 pN
HIV-1 type 0 [47]	G1-A63	10%	8 nt	Pseudoknot	12 pN
HIV-1 type B [19]	G1-U45	10%	1 nt	Stem-loop	19 pN

by the fact that the 0 frame system and the -1 frame system have the same extension of the spacer (=the end–end spatial distance between the A-site codon and the 5′ end of the downstream mRNA structure) at the frameshifting transition point.

For ScYLV in figure 1, frameshifting causes the anticodon–codon duplex to lose two Watson–Crick base pairs, resulting in a net loss of 1.7 kcal mol^{-1} in the codon–anticodon stability. In order to make the -1 frame thermodynamically favorable and hence likely to occur, the -1 frame must have lower free energy than the 0 frame. Mathematically, the thermodynamic condition for the transition between the two reading frames is determined by the free energy balance between the two systems (two frames):

$$\Delta G_{-1\,\text{frame}}(X^*) = \Delta G_{0\,\text{frame}}(X^*), \tag{7}$$

where X^* is the extension of the spacer when the -1 shifted frame and the original 0 frame becomes equally probable, $\Delta G(X)$ is the free energy for the ensemble of all the possible conformations of the three-component system, for the given extension X of the spacer (equation (1)).

The free energy profiles $\Delta G_{0\,\text{frame}}(X)$ and $\Delta G_{-1\,\text{frame}}(X)$ in figure 4 for the pseudoknot-promoted frameshifting systems (ScYLV, IBV and HIV-1 type O in figure 2) give the regions where the -1 frame is more stable than the 0 frame, so frameshifting would likely occur. However, it is important to note that equilibration between the 0 frame and the -1 frame is not necessarily established within the timescale of ribosomal pausing, and the 0 frame $\rightarrow$ -1 frame transition may not be driven by (equilibrium) spontaneous thermal fluctuation between the two frames. Therefore, X^* determined by equation (7) does not always correspond to the actual frameshifting transition point. As we show below, frameshifting is likely driven by the internal mechanical force in the system instead of the equilibrium thermal fluctuation between the two frames.

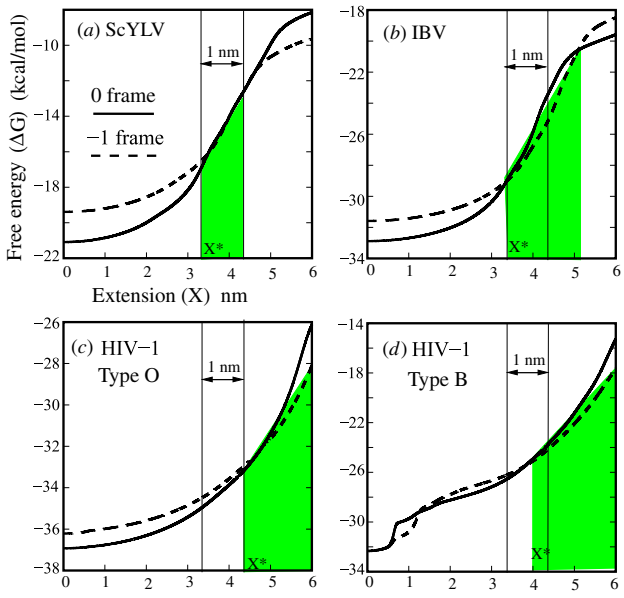

Figure 4. The free energy landscapes (profiles) for the 0 frame (solid line) and −1 frame (dashed line) for (*a*) ScYLV, (*b*) IBV, (*c*) HIV-1 type 0 and (*d*) HIV-1 type B. In the green regions, the −1 frame system is more stable than the 0 frame system. Also shown is the 1 nm (3.3 nm → 4.3 nm) frameshifting region. The region corresponds to the 9 Å movement proposed by Plant *et al* [16]. Frameshifting may occur during the period of the 9 Å movement.

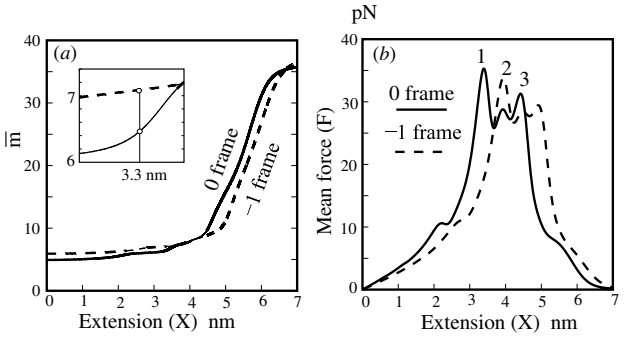

Figure 5. (*a*) The mean spacer length (=the mean number of the unpaired nucleotides in the 5′ end) and (*b*) the force (*F*)–extension (*X*) curve for the 0 frame and −1 frame of ScYLV. The inset of (*a*) shows the abrupt change of the mean spacer length at the transition point ($X = 3.3$ nm).

Stability of stem 1 in the downstream pseudoknot

We use ScYLV for illustration. The general conclusions below are valid for other pseudoknot-promoted −1 frameshifting systems that we have tested. The equilibrium transition point between the 0 frame and the −1 frame occurs at a spacer extension of $X^* = 3.3$ nm (figure 4(*a*)), which is also equal to the *X* value when frameshifting occurs (as determined from the tension force; see below). At the transition point, the mean number of the unpaired nucleotides in the spacer ($\overline{m}(X)$ in equation (5)) switches from $\overline{m}(X^*) = 6.5$ nt to 7.0 nt (figure 5(*a*)), resulting in an abrupt decrease in the mean distance between two adjacent bases from $X^*/\overline{m}(X^*) = 0.51$ nm to 0.47 nm. After the frameshifting transition, the spacer is less stretched and the tension is partially released. We note that $X^*/\overline{m}(X^*) = 0.51$ nm is close to the experimentally observed value 0.52 nm by Yusupova *et al* [16, 53].

Our structural calculations from $P_{ij}(X)$ (equation (6)) show that the pseudoknot structure in the 0 frame is partially unfolded at the transition point X^*: the terminal stack 6AA-UU23 of stem 1 is disrupted with nearly 100% probability, the next stack 7AG-CU22 is disrupted with only 50% probability, and all other base stacks remain intact (figure 2(*a*)). The base stack 7AG-CU22 hinders further unfolding of the RNA pseudoknot, causing the buildup of the tension in the spacer to induce frameshifting.

Stability of the codon–anticodon base pairs

Experiments indicated that changing the slippery sites from GGGAAAC to UUUAAAC for simian retrovirus type 1 (SRV-1) causes an increase in the frameshifting efficiency by 74% [32]. The increase in efficiency stems from the lowered 0 frame stability in the codon–anticodon region. Upon frameshift, the free energy ΔG_{codon} for the codon–anticodon base pairs increases. Such an increase is 0.3 kcal mol^{-1} smaller for UUUAAAC than for GGGAAAC. Thus, the relative probability between the −1 frame and the 0 frame for UUUAAAC is about $(e^{0.3 \text{ kcal mol}^{-1}/k_B T} - 1) \sim 66\%$ higher than for GGGAAAC at $T = 25\,^{\circ}$C. The results are close to the experimentally measured 74% increase in the frameshifting efficiency.

Maximum tension force and frameshifting transition

The tension force reaches its peak (35 pN) at the transition point X^* (figure 5(*b*)). The larger the maximum force, the more robust the pseudoknot, and the more likely frameshifting can occur. In addition, such a large force acts as an internal force to lower the kinetic barrier for the −1 ribosomal frameshifting and make frameshifting kinetically more favorable. Other factors can also play a role in the kinetics, such as the force from eEF2 during the translocation, which can affect the formation of tRNA–mRNA base pairing at the A-site [30, 31], and the GTP → GDP hydrolysis [54, 55] which can release about −7.3 kcal mol^{-1} energy [16], part of which can be used to promote the slippage.

The free energy condition for a thermodynamically favorable frameshifting is $\Delta G_{-1\,\text{frame}}(X) \leqslant \Delta G_{0\,\text{frame}}(X)$. The condition defines the regime of *X* (shaded regions in figure 4) where the −1 frame is more stable than the 0 frame. We find that the maximum (peak) force $F(X)$ usually occurs in such a regime of *X* and the force is larger for a larger free energy difference $\Delta G_{0\,\text{frame}}(X) - \Delta G_{-1\,\text{frame}}(X)$.

The 9 Å model [16] suggests that the codon–anticodon duplex moves toward the 5′ direction by a distance of about 1 nm, creating a tension in the spacer. Our crude estimation indicates that the average distance *X* of the spacer changes from about 3.3 nm to 4.3 nm during the process. Therefore, we will focus on the region of *X* between 3.3 nm and 4.3 nm. For several pseudoknot-induced frameshift, this region of *X* overlaps with the thermodynamically (figures 4(*a*) and (*b*)) accessible frameshifting regime. We call the tension force

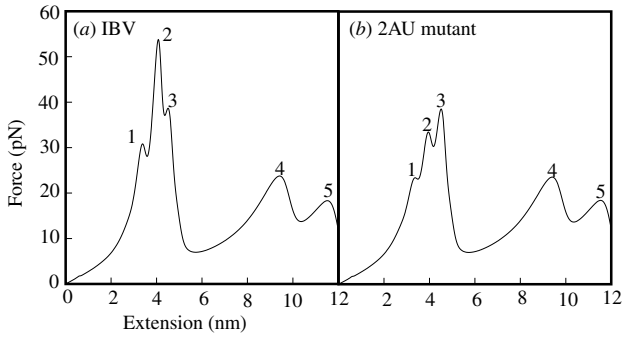

Figure 6. The force–extension curves for (*a*) the wild-type minimal IBV pseudoknot and (*b*) the mutant 2AU (8G-C35 → A-U). Peaks 1 and 2 for the 2AU mutant are notably suppressed. The suppression in the force may be correlated to the significant reduction in the frameshifting efficiency of the 2AU mutant.

(equation (4)) for X in the range between 3.3 nm and 4.3 nm as the 'frameshifting force'. Our computation with equation (4) shows that the frameshifting force–extension (X) curve usually shows three peaks. Our structural calculation from the base pairing probability ($P_{ij}(X)$ in equation (6)) indicates that the three force peaks correspond to the sequential breaking of the first three terminal base pairs in stem 1 of the pseudoknot.

For ScYLV, breaking the stable 7AG-CU22 base stack causes the largest maximum force (peak 1) of the tension prior to frameshifting. The frameshifting at $X^* = 3.3$ nm causes a great reduction in the tension force from 35 pN (0 frame) to a smaller value about 10 pN (−1 frame) (figure 5(*b*)). The release of the tension force in the spacer can result in partial refolding of the pseudoknot. Our structural calculations from $P_{ij}(X)$ (equation (6)) show that the 7AG-CU22 base stack, which is stable with 50% fractional population in the 0 frame, is now completely refolded (with nearly 100% fractional population) in the −1 frame. The refolding of the 7AG-CU22 base stack offsets the increase of the spacer length due to the frameshift, causing the spacer length $\overline{m}(X)$ to increase from 6.5 nt to 7.0 nt (difference = 0.5 nt < 1 nt) (figure 5(*a*)).

For a different virus, IBV, experimental results based on the minimal IBV pseudoknot (figure 2(*b*)) suggest that base pairs at the different positions of stem 1 play different intriguing roles in frameshifting. Weakening the second base pair (2AU mutation: 8G-C35 → A-U) causes a significant reduction in frameshifting efficiency from 48% to 18% [45]. In contrast, weakening the first base pair (1GG mutation [56]: 7G-C36 → G-G) or the fourth base pair (4AU mutation [45]: 10G-C33 → A-U) causes only minor reduction (10%) in frameshifting efficiency.

For the wild-type IBV (figure 5(*b*)), the frameshifting force of peak 2 (52 pN) at $X = 4.0$ nm for IBV (figure 6(*a*)) is much larger than that of peak 1 (30 pN) at $X = 3.3$ nm. The *Vfold* model [36] predicts that breaking the second base pair (8G-C35) involves a much larger free energy cost (ΔG = 3.4 kcal mol^{-1}) due to a smaller entropic gain for the pseudoknot loop than breaking the first base pair (7G-C36) ($\Delta G = 1.2$ kcal mol^{-1}). Therefore, peak 2 for the disruption of the second base pair has a much larger force than peak 1 for the disruption of the first base pair. We note that the largest $\Delta G_{0\,\text{frame}}(X) - \Delta G_{-1\,\text{frame}}(X)$ (and hence the most favorable frameshifting) (figure 4(*b*)) is at $X = 4.0$ nm, where peak 2 (figure 6(*b*)) occurs.

The 2AU mutant, which causes a 30% decrease in frameshifting efficiency from the wild-type IBV [45], shows a significant suppression in both peak 1 and peak 2 (figure 6(*b*)). This is because mutation of the second base pair concurrently destabilizes both the first and the second base stacks. The 1GG or the 4AU mutation, which causes only a 10% decrease in frameshifting efficiency [45, 56], shows only moderate suppression for one peak of the frameshifting force. Our calculations for other mutants also show correlation between the frameshifting force and the frameshifting efficiency. For instance, our calculations for mutants pKA13 (with shortened 10 bp stem 1) and pKA9 (with 9 bp in stem 1) (46, 59), which have low frameshifting efficiences of 7% and 2%, respectively, show significantly reduced frameshifting forces than the wild-type IBV. The 3AU mutation (figure 2(*b*)) causes a significant decrease in peaks 2 and 3 and is thus predicted to cause a large reduction in the frameshifting efficiency. In general, mutations beyond the third base pair have minor effects on the frameshifting forces and thus might affect the frameshifting efficiency weakly [45].

Frameshifting efficiency is not necessarily correlated to the thermodynamic stability. Probably more relevant to the frameshifting efficiency are the frameshifting forces. The pKA18 mutant of IBV [45] is $\Delta G = 7.1$ kcal mol^{-1} more stable than the wild-type IBV (figure 2(*b*)), but pKA18 and the wild-type IBV have the same frameshifting efficiency (48%). On the other hand, our calculations show that they have similar frameshifting forces: (30 pN, 52 pN and 37 pN) for the wild type and (34 pN, 52 pN, 34 pN) for pKA18. This example suggests a correlation between the frameshifting forces and the frameshifting efficiency. In summary, we find a reasonable correlation between the frameshifting force and the frameshifting efficiency; see figure 7 and table 1 for a summary. From the theoretical (force) and the experimental (efficiency) data, we fit a relationship between the frameshifting efficiency η and the mean force F_{avg} (between spacer extension $X_{\min} = 3.3$ nm and $X_{\max} = 4.3$ nm):

$$\eta \simeq 0.0083 e^{0.1 F_{\text{avg}}}. \tag{8}$$

The mean force F_{avg} is directly related to the work $\Delta W_{ss} = \int_{X_{\min}}^{X_{\max}} f_{\text{ss}}(X)\,\mathrm{d}X$ done by the tension force in the process:

$$F_{\text{avg}} = \Delta W_{ss}/(X_{\max} - X_{\min}). \tag{9}$$

The above analytical relationship is derived from theory-experiment tests for three series of mRNA sequences: ScYLV, IBV and its various mutants, and HIV-1 type O (table 1 and figure 7), which involve three different types of slippery sequences. As we discussed above, the codon–anticodon sequence in the slippery region can also affect the frameshifting efficiency. To examine the force–efficiency correlation for different sequences, we need to offset the effect arising from the different slippery sequences. As an extremely crude treatment, we choose IBV (slippery site: UUUUUUCA)

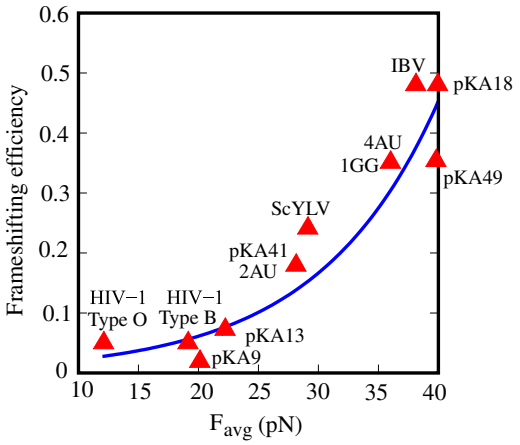

Figure 7. The correlation between the frameshifting efficiency and the peak forces within the range 3.3 nm $\leqslant X \leqslant$ 4.3 nm for the sequences that we have tested (see table 1). The figures show the correlation with the average force ($F_{\rm avg}$) in the range 3.3 nm $\leqslant X \leqslant$ 4.3 nm. The line shows the fitted analytical formula for the efficiency (η)–force relationship: $\eta \simeq 0.0083e^{0.1F_{\rm avg}}$. The symbols show the experimental data for the frameshifting efficiency. The frameshifting efficiencies were measured in the same translation system (Rabbit Reticulocyte Lysates). Different mRNAs can have different slippery sequences. To offset the effect arising from the differences in slippery sequences, we rescale the frameshifting efficiencies to account for the differences in the 0 frame $\rightarrow -1$ frame free energy changes for the codon–anticodon complexes. Specifically, we choose IBV and its mutants (pKA18, 1GG, 2AU, pKA41, 3AU, 4AU, pkA49, pKA13 and pKA9), which contain the same slippery sequence UUUAAAC, as the reference (without rescaling) and rescale the efficiencies for HIV-1 type O, which contain a different slippery sequence of UUUUUUA, by a factor of 0.43, and the efficiency for ScYLV, which contains slippery sequence GGGAAAC, by a scaling factor of 1.74 from the original experimental data [32].

as the reference case and rescale the frameshifting efficiencies for other sequences by a factor $p/p_{\rm IBV}$. Here, p is the fractional population of the -1 frame:

$$p = \frac{[-1]}{[0]+[-1]} = \frac{e^{-\Delta G^{(-1)}_{\rm codon}/k_{\rm B}T}}{e^{-\Delta G^{(-1)}_{\rm codon}/k_{\rm B}T} + e^{-\Delta G^{(0)}_{\rm codon}/k_{\rm B}T}} = \frac{e^{-\Delta\Delta G_{\rm codon}/k_{\rm B}T}}{e^{-\Delta\Delta G_{\rm codon}/k_{\rm B}T}+1},$$

and $p_{\rm IBV}$ is the p factor for IBV and $\Delta\Delta G_{\rm codon} = \Delta G^{(-1)}_{\rm codon} - \Delta G^{(0)}_{\rm codon}$ is the 0 frame $\rightarrow -1$ frame free energy change (of the codon–anticodon base pairs). For instance, HIV-1 type O contains a slippery sequence of UUUUUUA. $\Delta\Delta G_{\rm codon}$ is 0.5 kcal mol^{-1} smaller for UUUUUUA than for UUUAAAC (of IBV) and $p/p_{\rm IBV} \sim 0.43$ at $T = 25$ °C. Similarly, $p/p_{\rm IBV} \sim 1.74$ for ScYLV [32]. Figure 7 shows that the force for ScYLV is underestimated because we do not consider the loop-stem tertiary interactions. The tertiary interactions [29] can stabilize the native pseudoknot and hence strengthen the force during the movement of the codon–anticodon complex.

Figure 7 shows the correlation between the average force ($F_{\rm avg}$) and the frameshifting efficiency. The underlying mechanism for the correlation can be explained as the following. During the 3.3 nm $\rightarrow$ 4.3 nm process, the free energy change in the spacer region is equal to $\Delta W_{ss} = 1\ {\rm nm}\cdot F_{\rm avg}$ (equation (9)). This free energy buildup would lower the kinetic barrier for the subsequent breaking of the codon–anticodon base pairs (to induce the frameshift), contributing a factor $\sim e^{-\Delta W_{ss}/k_{\rm B}T}$ to the probability of frameshifting. Therefore, the frameshifting efficiency is correlated to the exponential of the average force $F_{\rm avg}$, specifically in the form of $e^{0.1F_{\rm avg}}$ (equation (8)). The factor 0.1 in the exponent is a result of the partition between the probability of breaking the codon–anticodon base pairs (frameshift) and of unfolding the downstream pseudoknot without frameshift.

Conclusion and outlook

By computing the free energy landscape for the three-component minimal frameshifting system (codon–anticodon pair, downstream mRNA structure and the spacer between them), we investigate the possible correlation between the force and the frameshifting efficiency. The model has the advantage of not having the artificial auxiliary RNA/DNA duplex handles used in the mechanical unfolding experiments. Our results suggest a correlation between the experimentally measured frameshifting efficiency and the tension force generated during the movement of codon–anticodon complexes. Moreover, our results suggest distinct spacer lengths for the frameshifting induced by the pseudoknot and by the stem-loop structure. The short spacer length in the stem-loop structure is due to the formation of the lower helix, which allows for a longer pausing time before the frameshifting occurs. The time for unzipping the lower helix may be crucial for efficient frameshifting. A brief summary of our findings are listed as follows.

(1) We find that the energetically favorable region for frameshifting occurs between $X = 3.3$ nm and $X = 4.3$ nm, where X is the spacer extension.
(2) Our results support the mechanical model of frameshifting. Specifically, we find that the frameshifting efficiency is correlated to the mean tension force $F_{\rm avg}$ between $X = 3.3$ nm and $X = 4.3$ nm.
(3) From extensive theory-experiment tests, we extract an analytical relationship between the frameshifting efficiency and the mean force $F_{\rm avg}$: $\eta \simeq 0.0083e^{0.1F_{\rm avg}}$

Although the results are supported by the recent experiments [30, 33], the present study probably addresses only a fraction of the complex frameshifting mechanism. For instance, the model cannot treat mRNA–ribosome interaction, which may be responsible for the effect of the length of stem 1 and the kink in the inter-helix junction region. Moreover, the predictions of the model are based on a 1 M NaCl salt condition; thus, they cannot account for the specific effect of the Mg^{2+} ions on the mRNA structure [58]. In addition, the model does not consider the loop-stem tertiary interactions [6, 29] and the kinetics [3, 7, 27], which are proposed to be important for several frameshifting systems. Nevertheless, the correlation between the frameshifting efficiency and the forces

as well as the stable frameshifting regions in the free energy landscape may provide a useful tool to predict frameshifting efficiency for a large class of frameshifting systems and may be useful for understanding the mechanical aspect of the frameshifting mechanism.

Glossary

(1) Retrovirus: virus consisting of an RNA genome which replicates via DNA through reverse transcription.
(2) −1 Frameshifting: a change in the translational reading frame such that the codon starts one nucleotide upstream from the original position in the messenger RNA sequence.
(3) Pseudoknot: an RNA tertiary motif where nucleotides in a loop form base pairs with complementary nucleotides outside the loop.

Acknowledgment

This work was supported by NIH through grant GM063732 (to S-J Chen).

References

[1] Jacks T and Varmus H E 1985 Expression of the Rous sarcoma virus pol gene by ribosomal frameshifting *Science* **230** 1237
[2] Jacks T, Madhani H D, Masiarz F R and Varmus H E 1988 Signals for ribosomal frameshifting in the Rous sarcoma virus gag-pol region *Cell* **55** 447
[3] Draper D E 1990 Pseudoknots and the control of protein synthesis *Curr. Opin. Cell. Biol.* **2** 1099
[4] Farabaugh P J 1996 Programmed translational frameshifting *Microbiol. Rev.* **60** 103
[5] Gesteland R F and Atkins J F 1996 Recoding: dynamic reprogramming of translation *Annu. Rev. Biochem.* **65** 741
[6] Kim Y C, Su L, Maas S, O'Neill A and Rich A 1999 Specific mutations in a viral RNA pseudoknot drastically change ribosomal frameshifting efficiency *Proc. Natl Acad. Sci.* **96** 14234
[7] Giedroc D P, Theimer C A and Nixon P L 2000 Structure, stability and function of RNA pseudoknots involved in stimulating ribosomal frameshifting *J. Mol. Biol.* **298** 167
[8] Baranov P V, Gesteland R F and Atkins J F 2002 Recoding: translational bifurcations in gene expression *Gene* **286** 187
[9] Brierley I and Dos Ramos F J 2006 Programmed ribosomal frameshifting in HIV-1 and the SARS-CoV *Virus Res.* **119** 29
[10] Brierley I, Pennell S and Gilbert R J C 2007 Viral RNA pseudoknots: versatile motifs in gene expression and replication *Nat. Rev. Microbiol.* **5** 598
[11] Jacks T, Townsley K, Varmus H E and Majors J 1987 Two efficient ribosomal frameshifting events are required for synthesis of mouse mammary tumor virus gag-related polyproteins *Proc. Natl Acad. Sci.* **84** 4298
[12] Dinman J D, Ruiz-Echevarria M J and Peltz S W 1998 Translating old drugs into new treatments: ribosomal frameshifting as a target for antiviral agents *Trends Biotechnol.* **16** 190
[13] Brierley I, Digard P and Inglis S C 1989 Characterization of an efficient coronavirus ribosomal frameshifting signal: requirement for an RNA pseudoknot *Cell* **57** 537
[14] Somogyi P, Jenner A J, Brierley I and Inglis S C 1993 Ribosomal pausing during translation of an RNA pseudoknot *Mol. Cell. Biol.* **13** 6931
[15] Kontos H, Napthine S and Brierley I 2001 Ribosomal pausing at a frameshifter RNA pseudoknot is sensitive to reading phase but shows little correlation with frameshift efficiency *Mol. Cell. Biol.* **21** 8657
[16] Plant E P, Jacobs K L, Harger J W, Meskauskas A, Jacobs J L, Baxter J L, Petrov A N and Dinman J D 2003 The 9 Å solution: how mRNA pseudoknots promote efficient programmed -1 ribosomal frameshifting *RNA* **9** 168
[17] Staple D W and Butcher S E 2005 Solution structure and thermodynamic investigation of the HIV-1 frameshift inducing element *J. Mol. Biol.* **349** 1011
[18] Gaudin C, Mazauric M H, Traikia M, Guittet E, Yoshizawa S and Fourmy D 2005 Structure of the RNA signal essential for translational frameshifting in HIV-1 *J. Mol. Biol.* **349** 1024
[19] Dulude D, Baril M and Brakier-Gingras L 2002 Characterization of the frameshift stimulatory signal controlling a programmed -1 ribosomal frameshift in the human immunodeficiency virus type 1 *Nucleic Acids Res.* **30** 5094
[20] Jacks T, Power M D, Masiarz F R, Luciw P A, Barr P J and Varmus H E 1988 Characterization of ribosomal frameshifting in HIV-1 gag-pol expression *Nature* **331** 280
[21] Du Z, Giedroc D P and Hoffman D W 1996 Structure of the autoregulatory pseudoknot within the gene 32 messenger RNA of bacteriophages T2 and T6: a model for a possible family of structurally related RNA pseudoknots *Biochemistry* **35** 4187
[22] Taylor E W, Ramanathan C S, Jalluri R K and Nadimpalli R G 1994 A basis for new approaches to the chemotherapy of AIDS: novel genes in HIV-1 potentially encode selenoproteins expressed by ribosomal frameshifting and termination suppression *J. Med. Chem.* **37** 2637
[23] Baril M, Dulude D, Steinberg S V and Brakier-Gingras L 2003 The frameshift stimulatory signal of human immunodeficiency virus type 1 group O is a pseudoknot *J Mol. Biol.* **331** 571
[24] Dinman J D, Richter S, Plant E P, Taylor R C, Hammell A B and Rana T M 2002 The frameshift signal of HIV-1 involves a potential intramolecular triplex RNA structure *Proc. Natl Acad. Sci.* **99** 5331
[25] Tinoco I Jr, Li P T and Bustamante C 2006 Determination of thermodynamics and kinetics of RNA reactions by force *Q. Rev. Biophys.* **39** 325
[26] Chen G, Wen J D and Tinoco I Jr 2007 Single-molecule mechanical unfolding and folding of a pseudoknot in human telomerase RNA *RNA* **13** 2175
[27] Green L, Kim C H, Bustamante C and Tinoco I Jr 2007 Characterization of the mechanical unfolding of RNA pseudoknots *J. Mol. Biol.* **375** 511
[28] Bidou L, Stahl G, Grima B, Liu H M, Cassan M and Rousset J P 1997 In vivo HIV-1 frameshifting efficiency is directly related to the stability of the stem-loop stimulatory signal *RNA* **3** 1153
[29] Cornish P V, Hennig M and Giedroc D P 2005 A loop 2 cytidine-stem 1 minor groove interaction as a positive determinant for pseudoknot-stimulated -1 ribosomal frameshifting *Proc. Natl Acad. Sci.* **102** 12694
[30] Namy O, Moran S J, Stuart D I, Gilbert R J and Brierley I 2006 A mechanical explanation of RNA pseudoknot function in programmed ribosomal frameshifting *Nature* **441** 244
[31] Léger L, ger M, Dulude D, Steinberg S V and Brakier-Gingras L 2007 The three transfer RNAs occupying the A, P and E sites on the ribosome are involved in viral programmed -1 ribosomal frameshift *Nucleic Acids Res.* **35** 5581

[32] ten Dam E, Brierley I, Inglis S and Pleij C 1994 Identification and analysis of the pseudoknot-containing Gag-Pro ribosomal frameshift signal of simian retrovirus-1 *Nucleic Acids Res.* **22** 2304
[33] Hansen T M, Reihani S N S, Oddershede L B and Sørensen M A 2007 Correlation between mechanical strength of messenger RNA pseudoknots and ribosomal frameshifting *Proc. Natl Acad. Sci.* **104** 5830
[34] Cao S and Chen S J 2005 Predicting RNA folding thermodynamics with a reduced chain representation model *RNA* **11** 1884
[35] Cao S and Chen S J 2006 Free energy landscapes of RNA/RNA complexes: with applications to snRNA complexes in spliceosomes *J. Mol. Biol.* **357** 292
[36] Cao S and Chen S J 2006 Predicting RNA pseudoknot folding thermodynamics *Nucleic Acids Res.* **34** 2634
[37] Serra M J and Turner D H 1995 Predicting thermodynamic properties of RNA *Methods Enzymol.* **259** 242
[38] Marck C and Grosjean H 2002 TRNomics: analysis of tRNA genes from 50 genomes of Eukarya, Archaea, and Bacteria reveals anticodon-sparing strategies and domain-specific features *RNA* **8** 1189
[39] Smith S B, Cui Y and Bustamante C 1996 Overstretching B-DNA: the elastic response of individual double-stranded and single-stranded DNA molecules *Science* **271** 795
[40] Strick T, Allemand J F, Croquette V and Bensimon D 2000 Twisting and stretching single DNA molecules *Prog. Biophys. Mol. Biol.* **74** 115
[41] Liphardt J, Onoa B, Smith S B, Tinoco I Jr and Bustamante C 2001 Reversible unfolding of single RNA molecules by mechanical force *Science* **292** 733
[42] Gerland U, Bundschuh R and Hwa T 2003 Mechanically probing the folding pathway of single RNA molecules *Biophys. J.* **84** 2831
[43] Gerland U, Bundschuh R and Hwa T 2004 Translocation of structured polynucleotides through nanopores *Phys. Biol.* **1** 19
[44] Hyeon C and Thirumalai D 2005 Mechanical unfolding of RNA hairpins *Proc. Natl Acad. Sci.* **102** 6789
[45] Napthine S, Liphardt J, Bloys A, Routledge S and Brierley I 1999 The role of RNA pseudoknot stem 1 length in the promotion of efficient -1 ribosomal frameshifting *J. Mol. Biol.* **288** 305
[46] Liphardt J, Napthine S, Kontos H and Brierley I 1999 Evidence for an RNA pseudoknot loop-helix interaction essential for efficient -1 ribosomal frameshifting *J. Mol. Biol.* **288** 321
[47] Baril M, Dulude D, Steinberg S V and Brakier-Gingras L 2003 The frameshift stimulatory signal of human immunodeficiency virus type 1 group O is a pseudoknot *J. Mol. Biol.* **331** 571
[48] Baril M, Dulude D, Gendron K, Lemay G and Brakier-Gingras L 2003 Efficiency of a programmed -1 ribosomal frameshift in the different subtypes of the human immunodeficiency virus type 1 group M *RNA* **9** 1246
[49] McCaskill J S 1990 The equilibrium partition-function and base pair binding probabilities for RNA secondary structure *Biopolymer* **29** 1105
[50] Chen S J 2008 RNA folding: conformational statistics, folding kinetics, and ion electrostatics *Annu. Rev. Biophys.* **37** 197
[51] Shen L X and Tinoco I Jr 1995 The structure of an RNA pseudoknot that causes efficient frameshifting in mouse mammary tumor virus *J. Mol. Biol.* **247** 963
[52] Walter A E and Turner D H 1994 Sequence dependence of stability for coaxial stacking of RNA helixes with Watson–Crick base paired interfaces *Biochemistry* **33** 12715
[53] Yusupova G Z, Yusupov M M, Cate J H and Noller H F 2001 The path of messenger RNA through the ribosome *Cell* **106** 233
[54] VanLoock M S, Agrawal R K, Gabashvili I S, Qi L, Frank J and Harvey S C 2000 Movement of the decoding region of the 16 S ribosomal RNA accompanies tRNA translocation *J. Mol. Biol.* **304** 507
[55] Moore P B and Steitz T A 2005 The ribosome revealed *Trends Biochem. Sci.* **6** 281
[56] Brierley I, Rolley N J, Jenner A J and Inglis S C 1991 Mutational analysis of the RNA pseudoknot component of a coronavirus ribosomal frameshifting signal *J. Mol. Biol.* **220** 889
[57] Plant E P and Dinman J D 2005 Torsional restraint: a new twist on frameshifting pseudoknots *Nucleic Acids Res.* **33** 1825
[58] Draper D E 2004 A guide to ions and RNA structure *RNA* **10** 335